



Quantitative analysis of sulfathiazole polymorphs in ternary mixtures by attenuated total reflectance infrared, near-infrared and Raman spectroscopy

Yun Hu^a, Andrea Erxleben^a, Alan G. Ryder^{a,b}, Patrick McArdle^{a,*}

^a School of Chemistry, National University of Ireland, Galway, Ireland

^b Nanoscale Biophotonics Laboratory, School of Chemistry, National University of Ireland, Galway, Ireland

ARTICLE INFO

Article history:

Received 7 December 2009

Received in revised form 30 April 2010

Accepted 4 May 2010

Available online 10 May 2010

Keywords:

Polymorphism

Sulfathiazole

NIR spectroscopy

ATR-IR spectroscopy

Raman spectroscopy

Partial least squares regression

ABSTRACT

The simultaneous quantitative analysis of sulfathiazole polymorphs (forms I, III and V) in ternary mixtures by attenuated total reflectance-infrared (ATR-IR), near-infrared (NIR) and Raman spectroscopy combined with multivariate analysis is reported. To reduce the effect of systematic variations, four different data pre-processing methods; multiplicative scatter correction (MSC), standard normal variate (SNV), first and second derivatives, were applied and their performance was evaluated using their prediction errors. It was possible to derive a reliable calibration model for the three polymorphic forms, in powder ternary mixtures, using a partial least squares (PLS) algorithm with SNV pre-processing, which predicted the concentration of polymorphs I, III and V. Root mean square errors of prediction (RMSEP) for ATR-IR spectra were 5.0%, 5.1% and 4.5% for polymorphs I, III and V, respectively, while NIR spectra had a RMSEP of 2.0%, 2.9%, and 2.8% and Raman spectra had a RMSEP of 3.5%, 4.1%, and 3.6% for polymorphs I, III and V, respectively. NIR spectroscopy exhibits the smallest analytical error, higher accuracy and robustness. When these advantages are combined with the greater convenience of NIR's "in glass bottle" sampling method both ATR-IR and Raman methods appear less attractive.

© 2010 Elsevier B.V. All rights reserved.

1. Introduction

Polymorphism is frequently defined as the ability of a substance to exist as two or more crystalline phases with different arrangements and/or molecular conformations in the crystal lattice [1]. It is widely observed in pharmaceutical compounds, and poses a significant problem for the pharmaceutical industry. Different polymorphs of a particular drug can exhibit different chemical and physical properties and thus show variation in solubility, dissolution rate, chemical reactivity, melting point, resistance to degradation, density and bioavailability [2–5]. Changes in these properties can dramatically alter both the therapeutic effect and processability of a drug. It is therefore important to establish reliable methods for the characterization of the solid-state forms of pharmaceutical products.

A number of techniques are available for the analysis of solid-state forms of pharmaceutical compounds. Some of the methods finding common use are X-ray powder diffraction (XRPD), differential scanning calorimetry (DSC), optical and electron microscopy, vibrational spectroscopy (including infrared (IR), near-infrared (NIR), and Raman methods) and more recently solid-state nuclear

magnetic resonance (NMR) has also been advocated [5–10]. In any specific case, the choice of technique depends on what is being investigated. However it is generally advisable to use two or more complementary methods to obtain a reliable knowledge of the solid forms [5]. It is well known that XRPD, perhaps the classic technique for analysis of the solid state and for the characterization of polymorphism, suffers from a range of problems including preferred crystal orientation, packing, and sample thickness [11–13]. These difficulties coupled with an ever-growing interest in fast, simple and reliable analytical methods have boosted the interest in vibrational spectroscopy.

Sulfathiazole (Fig. 1), a sulfa drug, is well known to exhibit at least five polymorphic forms. CCDC refcodes of the 5 characterized crystalline phases are suthaz01 (form I), suthaz (form II), suthaz02 (form III), suthaz04 (form IV) and suthaz05 (form V). The main differences between the polymorphs of sulfathiazole lie in hydrogen bonding and its effects on the arrangement of the molecules in the crystal lattice [14]. Sulfathiazole has been a model system for polymorphism research, thus, a wide array of research work has been reported [14–26]. The characterization and temperature-induced phase transitions of the five polymorphic forms of sulfathiazole have been studied in detail using magic-angle spinning NMR, DSC, terahertz pulsed spectroscopy, IR, and Raman spectroscopy [18–20]. It was also pointed out that the H bonding pattern in polymorph III in effect combines the ring system of II and IV. Con-

* Corresponding author. Tel.: +353 91 492487; fax: +353 91 525700.
E-mail address: p.mcardle@nuigalway.ie (P. McArdle).

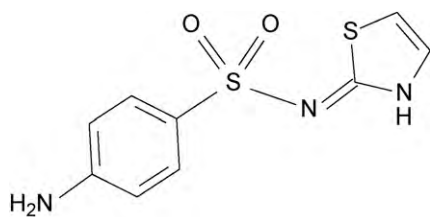


Fig. 1. Chemical structure of sulfathiazole.

sequently, the three polymorphs are very similar in all spectral and physicochemical behaviour [18]. It was not possible to obtain pure samples of forms II and IV as has already been reported by Apperley et al. [18]. It is likely that the close similarity of their crystal lattices is the reason, why they crystallize as mixtures. Pöllänen et al. [22,23] reported the use of in-line monitoring of the crystallization process of sulfathiazole. They also examined the combined use of IR, XRPD and multivariate data analysis. The effect of processing (crystallization, milling, tableting) on the polymorphism of sulfathiazole has also been investigated by NIR spectroscopy and thermal analysis [24]. The quantification of binary mixtures of forms I and III of sulfathiazole by NIR spectroscopy has also been reported [25,26].

The present study describes the simultaneous quantitative analysis of sulfathiazole polymorphs in ternary mixtures containing sulfathiazole forms I, III and V using ATR-IR, NIR and Raman spectroscopy. The experimental techniques used were evaluated for quantitation accuracy using partial least squares (PLS) analysis. The aim of this work was to determine which of the spectroscopic methods is the most accurate for the analysis of the solid-state forms of sulfathiazole. Density functional theory (DFT) B3LYP calculations and IR spectral simulation have been used to assign the vibrational modes. To reduce the effect of systematic variations, several spectral pre-processing methods, including standard normal variate (SNV), multiplicative scatter correction (MSC), first and second derivatives were applied to the data and their influences on the prediction errors were compared.

2. Material and methods

2.1. Materials

Sulfathiazole was purchased from Sigma–Aldrich with a purity of 98%, and was used as received. The commercial sulfathiazole was determined to be form III.

2.2. Methods

2.2.1. Sample preparation of the three polymorphic forms of sulfathiazole

Following the literature [17,25], form I was prepared by heating a commercial sulfathiazole sample in an oven for 30 min at 180 °C. Crystals of form V were obtained by evaporating a boiling aqueous solution of sulfathiazole to dryness, followed by drying at 105 °C [16]. Identification of polymorphs I and V and confirmation of their stability at ambient temperature were carried out by XRPD, as well as NIR spectroscopy. To minimize the particle size effect, the bulk samples of each form were milled using a planetary Micro mill (Pulverisette 7, Fritsch GmbH, Idar-Oberstein, Germany). XRPD was used to confirm that no polymorphic transformations occurred during milling.

2.2.2. Preparation of mixtures

Ternary polymorphic mixtures were prepared following a previously described procedure, Fig. 2 [27,28]. The mass ratios of polymorphs I, III and V were: (1:0:0), (0:1:0), (0:0:1), (2/3:1/3:0),

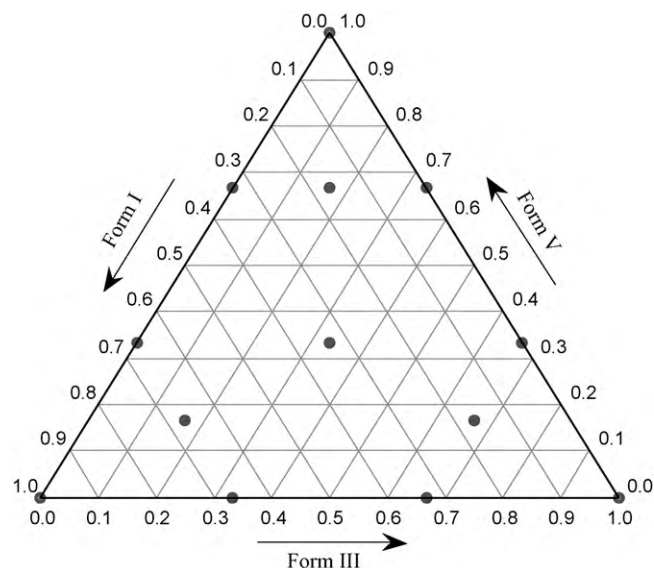


Fig. 2. Ternary diagram showing the composition of the 13 ternary mixtures consisting of different sulfathiazole polymorphs.

(2/3:0:1/3), (0:2/3:1/3), (0:1/3:2/3), (1/3:0:2/3), (1/3:2/3:0), (1/3:1/3:1/3), (2/3:1/6:1/6), (1/6:2/3:1/6), (1/6:1/6:2/3) (w/w/w). Physical mixtures (600 mg total for each mixture) were prepared and mixed uniformly for 3 min using a vortex mixer (Type 37600). All of the pure components and mixtures were sealed with Teflon-lined caps and kept in a desiccator at ambient temperature. XRPD was used to check their stability. The results showed that all samples were stable over the course of this work. Mixtures were prepared and analyzed in duplicate. In order to avoid possible systematic changes caused by instrumental and/or environmental fluctuations, samples were analyzed in a random manner immediately after preparation.

2.3. Analytical techniques

2.3.1. X-ray powder diffractometry

X-ray powder diffraction data were collected on a Siemens D500 powder diffractometer which was fitted with a diffracted beam monochromator. Diffraction patterns were recorded between 5° and 40° (2θ) using CuK_α radiation with steps of 0.05° with 2 s counting time per step. The Oscail software package was used to generate theoretical XRPD patterns of sulfathiazole polymorphs [29,30].

2.3.2. Attenuated total reflectance-infrared spectroscopy

ATR-IR spectra were recorded from 4000 to 650 cm⁻¹ using a PerkinElmer Spectrum 400 (FT-IR/FT-NIR Spectrometer) with 32 accumulations at a resolution of 4 cm⁻¹. This instrument was equipped with a DATR 1 bounce Diamond/ZnSe Universal ATR sampling accessory. Every sample was measured in triplicate and for each of the three measurements a fresh aliquot of sample was used.

2.3.3. Near-infrared spectroscopy

NIR spectra were collected in glass vials (15 mm × 45 mm) on a PerkinElmer Spectrum One fitted with an NIR reflectance attachment. Spectra were collected with interleaved scans in the 10,000–4000 cm⁻¹ range with a resolution of 8 cm⁻¹, using 32 co-added scans. Sample vials were shaken and repositioned between triplicate measurements of each sample.

2.3.4. Raman spectroscopy

Raman spectra were recorded at room temperature using a Raman spectrometer (AVALON Instruments Ltd, UK) equipped with

785 nm laser diode excitation and a cooled (-85°C) CCD detector. The system was fitted with a motorised XYZ sample stage. The samples were packed in disposable aluminum crucibles (Thorn Scientific Services Ltd, UK) of 2 mm depth and 5 mm diameter and measured with a laser power of 80 mW. An exposure time of $2\text{ s} \times 5$ scans was used for each measurement and spectra were collected over the Raman shift range of $250\text{--}3310\text{ cm}^{-1}$ with 4 cm^{-1} resolution. Each sample was analyzed on a 3×3 grid with 0.5 mm spacing. An average spectrum was calculated from the 9 points. For each mixture, three individual fresh samples were used in triplicate Raman measurements.

2.3.5. DSC measurement

DSC experiments were performed on a STA625 thermal analyzer from Rheometric Scientific. The heating rate was kept constant at $10^{\circ}\text{C min}^{-1}$ and all runs were carried out from 25°C to 250°C . The measurements were made in open aluminum crucibles, nitrogen was used as the purge gas in ambient mode, and calibration was performed using an indium standard.

2.3.6. Data analysis

Multivariate data analysis was carried out using the multivariate data analysis software The Unscrambler v.9.8 (Camo, Norway), PLS_Toolbox 4.0 (Eigenvector Research, Inc., US) and in-house-written Matlab routines. The calculations were performed using the MATLAB platform (The MathWorks, Inc., US) version 7.4 on a standard PC (2.8 GHz Pentium D Dell Optiplex PC, 1.0 GB RAM, Microsoft Windows XP OS). The Savitzky-Golay first and second derivatives were performed with a window size of 11 points and second order polynomial.

The preparation of each mixture in duplicate generated a total of 78 spectroscopic measurements for each spectroscopic method. Then according to the mass ratios of the polymorphs in the mixtures these measurements were sorted in one matrix. To avoid bias every set of measurements was split into a calibration set and a prediction set. Thus, the range of concentrations of polymorphic form I, III and V in calibration set covered the range in the prediction set and the distribution of the samples was appropriate in both calibration and prediction sets. The spectroscopic data were subjected to mean centering prior to PLS analysis. The optimal number of PLS factors (or latent variables, LVs) was determined by using a leave-one-out cross validation procedure. One single model was developed for each calibration set of the three polymorphs. The performance of the model provided by the different pre-processing methods was evaluated by using the correlation coefficient (R^2) and root mean square error (RMSE) of the residuals obtained with the PLS model, defined as

$$\text{RMSE} = \sqrt{\frac{\sum_{i=1}^n (y_i - \hat{y}_i)^2}{n}}$$

where y_i is the reference value, \hat{y}_i the calculated value and n is the number of samples. RMSE is termed root mean square error of calibration (RMSEC) for the calibration set, and root mean square error of prediction (RMSEP) for the prediction set.

2.4. Theoretical infrared analysis

Theoretical infrared analysis calculations were carried out in order to more fully understand the spectroscopic differences that arise in the ATR-IR spectra of the pure polymorphs and to enable vibrational assignment of these differences. All calculations were performed using the PC GAMESS/Firefly package [31] which is partially based on the GAMESS (US) source code [32]. The density functional theory method B3LYP was used with a 6-31G* basis set. The PC GAMESS program was driven by the molecular mod-

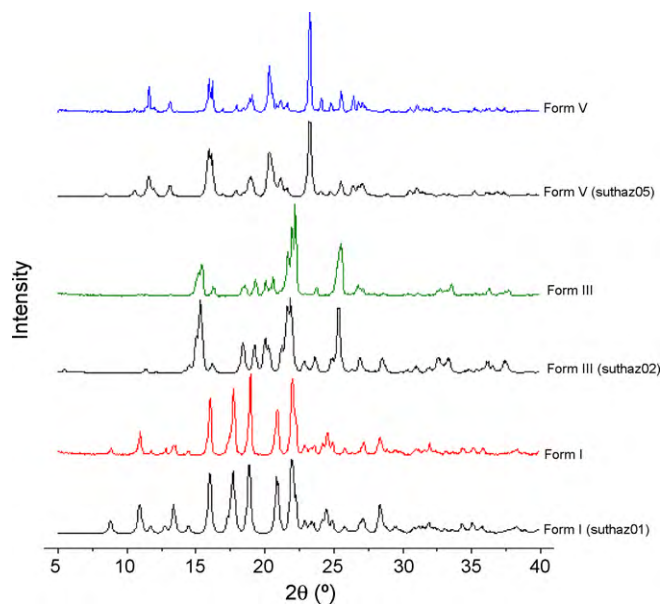


Fig. 3. Theoretical (suthaz01, suthaz02 and suthaz05) and experimental XRPD patterns of the three polymorphic forms (I, III and V) of sulfathiazole.

elling functionality (Moilin) within the Oscail software package [29]. Moilin was also used to animate the vibrational modes.

3. Results and discussion

3.1. Characterization of the three polymorphs of sulfathiazole

The polymorphic forms (I, III, and V) of sulfathiazole were characterized by XRPD (Fig. 3), ATR-IR (Fig. 4), NIR and Raman (Fig. 5) spectroscopy. It is clear that the XRPD patterns and the spectra of the three polymorphs show clear differences and that these techniques are suitable for qualitative and quantitative analysis.

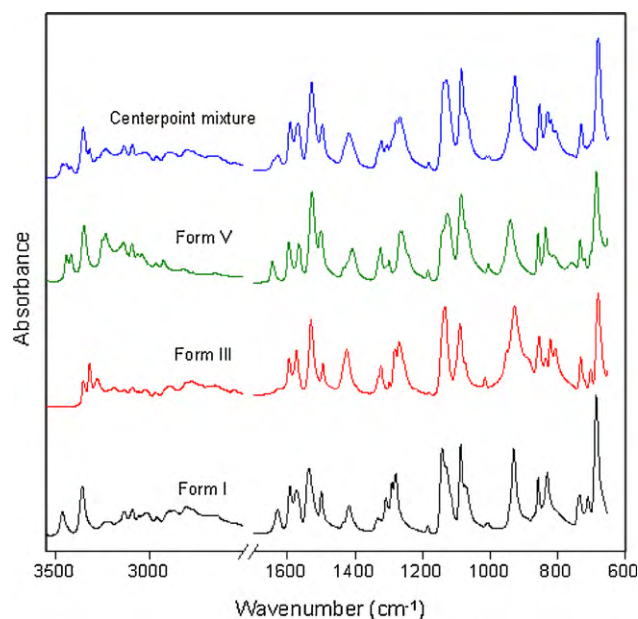


Fig. 4. ATR-IR spectra of the three polymorphic forms (I, III and V) of sulfathiazole and a ternary mixture consisting of equal amounts of the three single components.

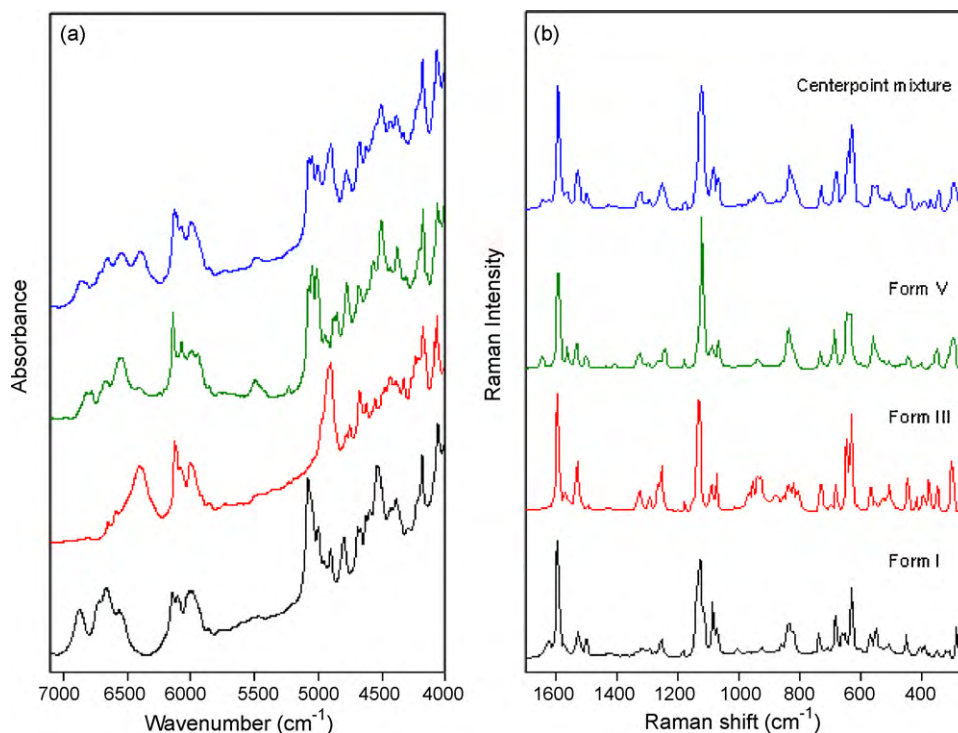


Fig. 5. (a) NIR and (b) Raman spectra of the three polymorphic forms of sulfathiazole and a ternary mixture consisting of equal amounts of the three single components.

3.1.1. XRPD

The crystal structures of the sulfathiazole polymorphs (forms I, III and V) were verified by comparing observed XRPD patterns with those calculated using the structures available on the Cambridge Crystallographic Data Centre (CCDC), Fig. 3. For example, the XRPD pattern of form I is distinguished by a 2θ peak at 10.9° , together with peaks at 16.0° , 17.7° , 18.8° , 20.9° and 21.9° . The peaks at 20.3° and 23.3° are specific for form V [16,26]. In contrast, in the XRPD pattern of sulfathiazole form III significant intensity differences are observed between the calculated and experimental pattern due to preferred crystal orientation effects. This makes the spectroscopic methods more appropriate for quantitative purposes than XRPD. DSC experiments (data not presented) further confirmed the identity of the polymorphs. Thus the thermogram of form I does not show any transformation prior to melting around 202°C , and that of form III shows transformation into form I at a temperature around 166°C prior to melting as transformed I. Form V displays two overlapping melting peaks around 200°C .

It was also essential to establish that the preparative methods used gave pure samples of each polymorph. It was possible to repeat and confirm some of the methods reported in the literature. Pure form I could be easily made in a reliable and reproducible way by heating commercial sulfathiazole samples at 180°C for 30 min in an oven [18]. Pure form V can be obtained by boiling an aqueous sulfathiazole solution to dryness. However, it is essential that form V be held at 100°C until dry as if the temperature drops before the sample is dry residual water appears to catalyse the transformation of form V to form I, to form III or to mixtures of forms III and IV [16,17,19]. Form V prepared as described here was stable over the course of this study (*cf* experimental section).

3.1.2. ATR-FTIR spectroscopy

In contrast to X-ray diffraction IR cannot provide any direct structural information. However, spectroscopic variations associated with each polymorph, which arise from changes in intramolecular hydrogen bonding, are observed. The ATR-IR spec-

tra of the three polymorphic forms of sulfathiazole are shown in Fig. 4. Furthermore, spectra obtained by mathematical addition of pure polymorph spectra closely matched those observed for mixtures [33]. In the IR spectra of sulfathiazole polymorphs, the first interesting region is $3500\text{--}3200\text{ cm}^{-1}$, as it is here that any differences in H-bonding will have greatest effect. Each phase has specific bands in the NH stretching vibration region (Fig. 4). The spectra were assigned using a theoretical spectrum calculated for sulfathiazole in the gas phase using PC GAMESS. The vibrational modes were assigned using vibrational animation (Table 1). A scale factor of 0.96 was used as the calculated vibrational frequencies may be expected to differ from experimental values due to the neglect of anharmonicity.

It is clear from Table 1 that the characteristic fundamental bands of form I corresponding to the N–H stretching vibrations at 3464 and 3358 cm^{-1} are shifted to lower wavenumber (3320 and 3280 cm^{-1}) in form III due to the increased intermolecular hydrogen bonding present [25,26]. For form V, the peak at highest wavenumber is divided into two overlapping bands at 3443 and 3418 cm^{-1} . Each polymorph also exhibits a characteristic spectrum in the IR fingerprint region ($1800\text{--}650\text{ cm}^{-1}$). Generally, the bands corresponding to the δNH_2 vibration can be observed at $1650\text{--}1590\text{ cm}^{-1}$. Polymorphs III and V have δNH_2 vibrations at 1628 , 1594 and 1644 , 1596 cm^{-1} , respectively. On the other hand, polymorph I has δNH_2 vibrations at 1634 , 1627 and 1592 cm^{-1} . The wagging NH_2 mode for the three polymorphs is observed around 730 cm^{-1} . The bands around 1323 and 1128 cm^{-1} are assigned to asymmetric and symmetric stretching vibrations of SO_2 . In addition, the IR spectra show a strong band around 1530 cm^{-1} , attributed to the stretching vibration of $\text{C}=\text{N}$ of the thiazole ring.

It is clear from this discussion that there are spectral features associated with each polymorph. However, the characteristic absorption bands are widely distributed in the IR spectra and therefore a multivariate calibration approach for the quantitative analysis of mixtures of the three polymorphs is likely to be more successful.

Table 1
Observed and calculated frequencies for sulfathiazole polymorphs I, III, V between 3700 and 650 cm⁻¹.

Calculated (cm ⁻¹)	Band assignment	Polymorph I observed (cm ⁻¹)	Polymorph III observed (cm ⁻¹)	Polymorph V observed (cm ⁻¹)
3550	$\nu_{as}(\text{NH}_2)$	3464	3320	3443, 3418
3442	$\nu_s(\text{NH}_2)$	3358	3280	3348
3319	$\nu(\text{NH})$			
3164	$\nu(\text{CH})$	3136	3136	3140
3131	$\nu(\text{CH})$	3116	3116	3117
3105	$\nu(\text{CH})$	3094	3093	3096
3073	$\nu(\text{CH})$	3072	3074	
3064	$\nu(\text{CH})$	3058	3058	3064
3031	$\nu(\text{CH})$	3014	3024	3041
1607	$\delta(\text{NH}_2)$	1634, 1627	1628	1644
1586	$\delta(\text{NH}_2) + \nu_{\text{ring}}(\text{phenyl})$	1592	1594	1596
		1574	1573	1566
1577	$\nu(\text{C}=\text{N})(\text{thiazole})$	1534	1530	1526
1567	$\nu(\text{CC})(\text{thiazole})$	1499	1495	1500
1481	$\delta(\text{CH})(\text{phenyl}) + \nu(\text{C}-\text{NH}_2)$	1417	1424	1407
1224	$\nu_{as}(\text{SO}_2)$	1334	1323	1324
1174	$\delta(\text{CH}) + \delta(\text{CNC})$	1290	1280	1299
1159	$\delta(\text{CH})(\text{phenyl})$	1279	1268	1259
1107	$\delta(\text{CH})(\text{phenyl})$	1184	1179	1184
1011	$\nu_s(\text{SO}_2)$	1128	1133	1125
1087	$\nu(\text{C}-\text{S}) + \delta(\text{CH})$	1086	1088	1084
1081	$\delta(\text{CH}) + \delta(\text{NH}) + \nu(\text{C}-\text{S})$	1073	1072	1069
1049	$\delta(\text{CH}) + \delta(\text{NH})$	1007	1013	1004
916	$\gamma(\text{CH})(\text{phenyl})$	929	927	939
816	$\gamma(\text{CC})$	857	853	856
800	$\gamma(\text{CH})$	829	833	834
700	$\omega(\text{NH})$	734	730	732
694	$\gamma(\text{CC})(\text{phenyl})$	684	678	683

Vibrational modes— ν : stretching; δ : in-plane deformation; γ : out-of-plane deformation; ω : wagging. Subscripts: s: symmetric; as: asymmetric.

3.1.3. NIR spectroscopy

NIR spectroscopy has extensive applications in the characterization of the physical state and quantitative analysis of polymorph mixtures. Indeed NIR spectroscopy has important advantages over traditional IR spectroscopy, such as simpler sample preparation, lack of a concentration limit and more accurate intensity measurements. The bands observed in NIR spectra have their origin in vibrational overtone and combination modes and are thus less suitable for direct identification purposes than IR spectra. Fig. 5a shows NIR spectra of the three crystal forms of sulfathiazole in the 7100–4000 cm⁻¹ region. Clear spectral differences are apparent, especially between 7050–5820 and 5150–4850 cm⁻¹ [24]. The largest differences are observed in the 7050–5820 cm⁻¹ region, which encompasses the region where the first overtones of the N–H stretching vibrations are expected. The bands in this region for form III are shifted to lower wavenumber compared to those of forms I and V which reflects the changes in hydrogen bonding observed in the IR. In forms I and V one of the NH₂ hydrogens is not involved in hydrogen bonding whereas in form III both amino hydrogens are involved in hydrogen bonding. The same phenomenon can be observed in the 5150–4850 cm⁻¹ region, which corresponds to the combination of the N–H stretching and bending vibrations. These NIR band assignments are in general agreement with those reported in the literature [25,34]. When compared to IR spectra the NIR spectra are much more sensitive to polymorph differences. This is in line with results for other systems where NIR gave lower RMSEP values than IR spectroscopy [35]. It is thus possible to achieve accurate low content quantification of sulfathiazole form I (0–5%) in binary mixtures with form III using NIR spectroscopy [26].

3.1.4. Raman spectroscopy

Raman spectroscopy has distinct advantages in the analysis of solid materials because of the minimal sample preparation required and the non-contact, non-destructive nature of the measurement. Like IR and NIR spectroscopy, Raman spectroscopy gives different physical forms their unique spectral features due to differ-

ences in vibrational energy and changes in molecular polarizability. Raman spectroscopy shows stronger spectral intensity for aromatic molecules and molecules containing polarizable atoms. It is also less sensitive to the presence of water. Furthermore, particle size effects can be counteracted by the use of special sampling techniques [27,36]. Lee et al. have successfully used Raman microscopy to identify the polymorphs of sulfathiazole that nucleated on patterned substrates [37].

The Raman spectra of forms I, III, and V are shown in Fig. 5b. There are clear differences especially at 1600 cm⁻¹ and between 1000–800 cm⁻¹. For example while all the three forms have differences close to 1600 cm⁻¹, polymorph I has two overlapping bands around 1630 cm⁻¹, polymorph V has a single band at 1645 cm⁻¹ and polymorph III has no band in this region. The strongest Raman bands of the three forms are due to the SO₂ stretching vibrations and the ring deformation modes at 1132 and 632, 1128 and 631, 1122 and 635 cm⁻¹ for polymorph forms I, III and V, respectively. Recently an assignment of the Raman bands of forms I and III has been reported [34].

3.2. Quantification by ATR-FTIR, NIR and Raman spectroscopy

While as described above, the IR, NIR and Raman spectra of the three sulfathiazole polymorphs are different, the aim here was to determine which technique gave the most accurate quantitation of the three polymorphs (I, III, V). Since the spectra do not show a single relatively intense peak that is characteristic of each polymorph the chemometric method is likely to be more successful than univariate techniques. Partial least squares analysis (PLS) was applied to the following spectral regions: for IR spectra from 1700 to 650 cm⁻¹, for NIR spectra from 7050 to 5820 and 5150 to 4000 cm⁻¹, and for Raman spectra the 1698 to 602 cm⁻¹ region was used.

For solid samples the systematic variation is due to, among others, light scattering and differences in pathlength, and may often constitute the major part of the variation of the sample spectra. Thus, pre-processing the data before spectral calibration is often

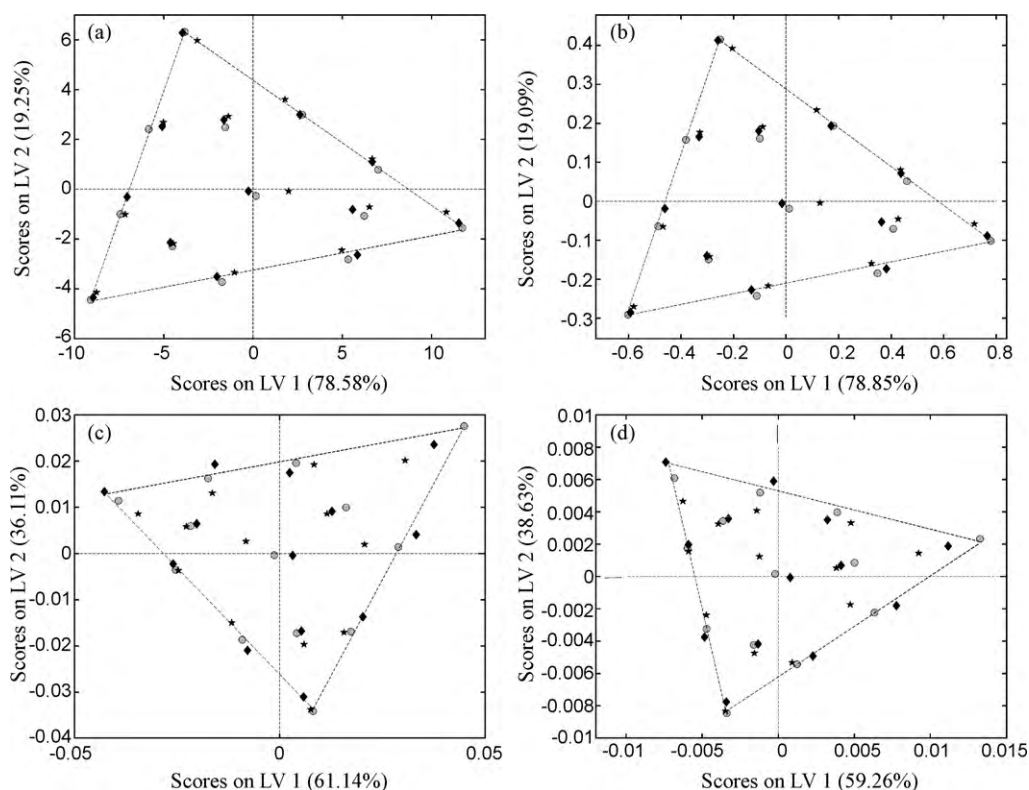


Fig. 6. Score plots generated by PLS models with different pre-processing methods (a) SNV, (b) MSC, (c) 1st derivative, (d) 2nd derivative from NIR data (7050–5820 and 5150–4000 cm^{-1}). ●, ◆, ★ represent three different measurements of each individual sample mixture.

employed in order to reduce the effect of systematic variations, which are not related to the measured parameters [38]. In this study, four different pre-processing methods, including multiplicative scatter correction (MSC), standard normal variate (SNV), first derivative, and second derivative were applied. These methods are often used to remove unimportant baseline (offset) interferences from samples or correct scatter effects and accentuate spectral signals of interest. Fig. 6 shows the score plots generated by PLS with the different pre-processing methods from NIR data. Overall, the triangular shape of the experimental design (Fig. 2) could be observed in these score plots. The score plots obtained following MSC and SNV pre-treatment show the best clustering. On the other hand, three different measurements of each individual sample mixture cluster tightly to each other, which indicates that the variations between the NIR spectra subjected to both the SNV and MSC procedures are smaller than those derived from first and sec-

ond derivatives. For the latter, a slight spreading of the scores within clusters can be observed on the score plots (Fig. 6c and d). The prediction results of PLS models developed from the pre-processed data are listed in Table 2. It can be observed that both the SNV and MSC led to simpler PLS models (less PLS factors) with rather smaller RMSEC and RMSEP values in all cases. The relative success of the MSC and SNV performance is due to their ability to minimize light scattering effects by removal of offsets and slopes in the spectra caused by the light scattering intrinsic to solid samples [39]. In contrast first and second derivative pre-treatments which are often effective in the amplification of weak sharp peaks at the expense of broad peaks or changes in the baseline in this study appear to do little more than enhance noise. Therefore, while using first and second derivatives for pre-processing does accentuate signals of interest due to their inherent higher rates of change, it does not deal with scattering effects. Consequently, scattering effects

Table 2

Performance of PLS quantification results for ATR-IR (1700–650 cm^{-1}), NIR (7050–5820 cm^{-1} and 5150–4000 cm^{-1}) and Raman (1698–602 cm^{-1}) data using different pre-processing methods.

Spectroscopy	Pre-processing method	PLS factors	Form I		Form III		Form V	
			RMSEC %	RMSEP %	RMSEC %	RMSEP %	RMSEC %	RMSEP %
ATR-IR	MSC	2	4.4	5.0	5.5	5.0	5.1	4.6
	SNV	2	4.4	5.0	5.5	5.1	4.8	4.5
	1 st derivative	3	5.2	6.8	5.1	5.7	5.8	5.8
	2 nd derivative	3	5.2	6.7	5.0	5.5	6.0	6.1
NIR	MSC	2	2.0	2.0	3.1	2.8	3.1	2.9
	SNV	2	2.0	2.0	3.2	2.9	3.0	2.8
	1 st derivative	2	3.6	4.6	5.1	5.2	5.1	6.1
	2 nd derivative	2	4.1	5.1	4.6	4.5	4.9	6.2
Raman	MSC	2	2.5	3.4	3.5	4.0	2.9	3.5
	SNV	2	2.8	3.5	3.3	4.1	3.0	3.6
	1 st derivative	3	4.2	5.5	4.2	5.9	3.8	4.9
	2 nd derivative	3	4.1	5.5	4.3	6.0	3.8	4.9

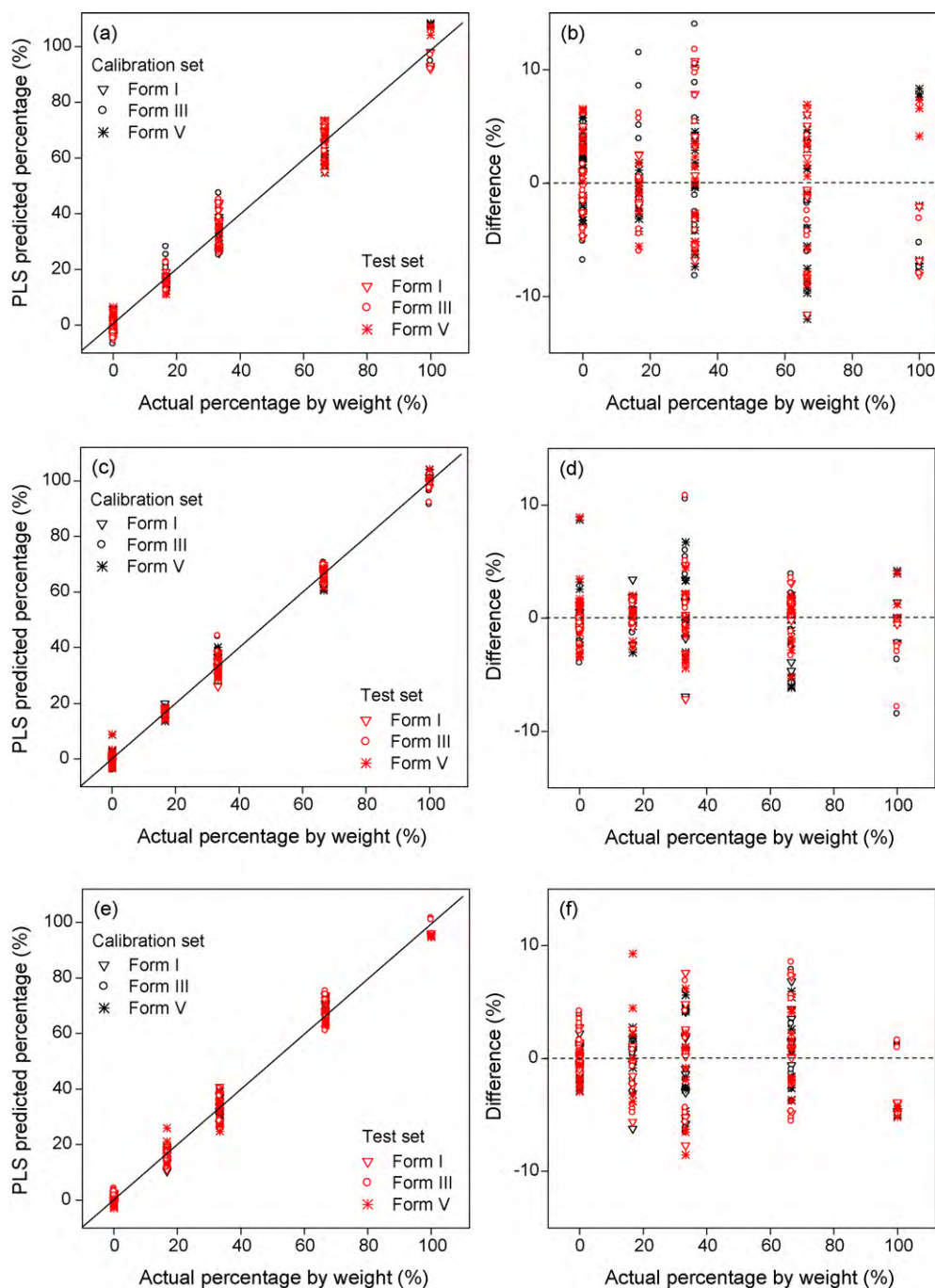


Fig. 7. Predicted vs. actual percentage by weight and the distribution of residuals from the model based on (a, b) ATR-IR (1700–650 cm⁻¹), (c, d) NIR (7050–5820 cm⁻¹ and 5150–4000 cm⁻¹) and (e, f) Raman (1698–602 cm⁻¹) data.

appear as an additional PLS factor. The equations for the SNV and MSC transformations have the same form and, in many cases, the two approaches produce very similar results so that they are widely regarded as exchangeable [40,41]. However, the advantage of SNV over MSC is that SNV is applied to an individual spectrum, whereas MSC uses a reference spectrum.

Fig. 7 shows the multivariate calibration curves and the relative errors calculated for the IR, NIR and Raman measurements using the SNV and PLS algorithms with two latent variables. A good linear relationship was observed between the actual and predicted concentrations for calibration standards for all three polymorphs in these three measurements. The correlation coefficients (R^2) of IR, NIR and Raman measurements are respectively: 0.9799, 0.9691

and 0.9769 for polymorph I, 0.9959, 0.9898 and 0.9906 for polymorph III and 0.9923, 0.9886 and 0.9910 for polymorph V. The root mean square errors of calibration (RMSEC), Table 2, calculated for the IR, NIR and Raman spectra with SNV pre-treatment were: 4.4, 5.5 and 4.8; 2.0, 3.2 and 3.0; and 2.8, 3.3, 3.0%, respectively for forms I, III and V. The PLS prediction errors (RMSEP) showed small values of: 5.0, 5.1 and 4.5; 2.0, 2.9 and 2.8; and 3.5, 4.1, and 3.6% for forms I, III and V respectively. The results indicated that NIR shows slightly smaller RMSECs and RMSEPs than Raman and ATR-IR. It is also clear that the relative errors calculated from ATR-IR data are higher values than those from NIR and Raman measurements.

To further evaluate these techniques, we also carried out error analysis on each technique by calculating the relative standard

Table 3

Assessment of influence of potential sources of error on ATR-IR, NIR and Raman spectroscopy.

Source of error	IR spectroscopy R.S.D. (%) ^a			NIR spectroscopy R.S.D. (%) ^a			Raman spectroscopy R.S.D. (%) ^a		
	F I	F III	F V	F I	F III	F V	F I	F III	F V
Instrument reproducibility	0.3	0.3	0.2	0.3	0.2	0.6	1.3	0.2	1.0
Intra-day variability	0.8	0.7	0.5	0.9	0.3	0.5	1.1	1.2	2.7
Inter-day variability	3.5	3.0	1.9	1.7	1.3	0.6	7.6	3.1	4.1

^a PLS models using SNV pre-processing.

deviation (RSD) when the PLS models based on SNV pre-processing were applied, as shown in Table 3. On the whole, the RSD values for instrument reproducibility, intra-day variability and inter-day variability of IR and NIR are slightly better than for Raman spectroscopy. Generally, parameters involving the response of the instrument with no sample disturbance (instrument reproducibility and intra-day variability) gave relatively small RSD values (around 2%) indicating good reproducibility of the technique [42]. A possible explanation for the higher inter-day variability of Raman and IR spectroscopies is the lack of control over laboratory temperature and/or humidity. NIR is less susceptible to environmental changes, as the samples were kept in closed vials.

Sample homogeneity is very important in the quantification of solid mixtures and while control of sample mixing will always be a problem it does appear from this work that NIR spectra are less susceptible to mixing problems than IR and Raman methods. It has been pointed out that the major source of quantification error in ATR-IR and Raman methods comes from the small sampling size [43]. In an attempt to reduce these problems Raman measurements were made on three independent samples and nine measurements were performed on each sample to reduce small sampling size errors. The IR sampling area was 1 mm in diameter and special care was taken to reproduce the applied sample pressure. NIR spectra were collected in glass sample vials and the spectra were recorded from a sample area which was 15 mm in diameter. Measuring each sample in triplicate also contributed to the reduction of sampling errors arising from inhomogeneity.

In summary, for the quantification of sulfathiazole polymorphs I, III and V in ternary mixture NIR spectroscopy is the most reliable method. To further assess the usefulness of NIR spectroscopy for the analysis of ternary sulfathiazole mixtures the limits of detection (LOD) and limits of quantification (LOQ) have been calculated. LOD and LOQ were determined using blank samples and $LOD = 3.3 \times \sigma/s$ (σ = standard deviation; s = slope of the calibration plot) [44] and $LOQ = 10 \times \sigma/s$ [45]. The standard deviations for the SNV pre-treatment model were 1.09, 1.74 and 1.90% for forms I, III and V, respectively. Thus the LOD and LOQ values for the NIR analyses were 3.6 and 10.9% for form I, 5.8 and 17.6% for form III and 6.3 and 19.0% for form V. These results are in the same range as those reported for other ternary polymorph analyses [46].

4. Conclusions

In this study, vibrational spectroscopy (ATR-IR, NIR and Raman spectroscopy) in conjunction with partial least squares (PLS) has been successfully applied to the simultaneous quantitation of sulfathiazole polymorphic forms (I, III and V) in ternary mixtures. These techniques are fast and non-destructive, and relatively easy to use. The performance of models developed using four spectral pre-treatment methods, SNV, MSC, first and second derivatives was compared. From a comparison of the predictive performance of each measurement and error analysis it was found that NIR spectroscopy exhibits higher accuracy, robustness and ease of use over Raman and ATR-IR methods. To reduce the effect of the small laser spot size in the Raman measurements and to improve the quantification results it was necessary to collect and average spectra from

different positions within the sample. The present results may provide a useful insight into the effectiveness of spectroscopic methods for polymorph analysis.

Acknowledgements

The authors thank Science Foundation Ireland (SFI) for funding for Solid State Pharmaceuticals Cluster (SSPC). Mr. Dermot McGrath is thanked for DSC measurements.

References

- [1] D.J.W. Grant, Theory and origin of polymorphism, in: H.G. Brittain (Ed.), *Polymorphism in Pharmaceutical Solids*, Informa Healthcare USA, Inc., New York, 2007, pp. 1–34.
- [2] A.S. Raw, L.X. Yu, Pharmaceutical solid polymorphism in drug development and regulation, *Adv. Drug Deliv. Rev.* 56 (2004) 235–236.
- [3] S. Datta, D.J.W. Grant, Crystal structures of drugs: advances in determination, prediction and engineering, *Nat. Rev. Drug Dis.* 3 (2004) 42–57.
- [4] A. Llinàs, J.M. Goodman, Polymorph control: past, present and future, *Drug Dis. Today* 13 (2008) 198–210.
- [5] J. Aaltonen, M. Allesø, S. Mirza, V. Koradia, K.C. Gordon, J. Rantanen, Solid form screening—a review, *Eur. J. Pharm. Biopharm.* 71 (2009) 23–37.
- [6] D.E. Bugay, Characterization of the solid-state: spectroscopic techniques, *Adv. Drug Deliv. Rev.* 48 (2001) 43–65.
- [7] G.A. Stephenson, R.A. Forbes, S.M. Reutzel-Edens, Characterization of the solid state: quantitative issues, *Adv. Drug Deliv. Rev.* 48 (2001) 67–90.
- [8] A.W. Newman, S.R. Byrn, Solid-state analysis of the active pharmaceutical ingredient in drug products, *Drug Dis. Today* 8 (2003) 898–905.
- [9] B. Shan, V.K. Kakumanu, A.K. Bansal, Analytical techniques for quantification of amorphous/crystalline phases in pharmaceutical solids, *J. Pharm. Sci.* 95 (2006) 1641–1665.
- [10] J. Aaltonen, K.C. Gordon, C.J. Strachan, T. Rades, Perspectives in the use of spectroscopy to characterise pharmaceutical solids, *Int. J. Pharm.* 364 (2008) 159–169.
- [11] S.N.C. Roberts, A.C. Williams, I.M. Grimsey, S.W. Booth, Quantitative analysis of mannitol polymorphs. X-ray powder diffractometry - exploring preferred orientation effects, *J. Pharm. Biomed. Anal.* 28 (2002) 1149–1159.
- [12] M. Varasteh, Z. Deng, H. Hwang, Y.J. Kim, G.B. Wong, Quantitative determination of polymorphic impurity by X-ray powder diffractometry in an OROS® formulation, *Int. J. Pharm.* 366 (2009) 74–81.
- [13] F. Tian, F. Zhang, N. Sandler, K.C. Gordon, C.M. McGoverin, C.J. Strachan, D.J. Saville, T. Rades, Influence of sample characteristics on quantification of carbamazepine hydrate formation by X-ray powder diffraction and Raman spectroscopy, *Eur. J. Pharm. Biopharm.* 66 (2007) 466–474.
- [14] N. Blagden, R.J. Davey, H.F. Lieberman, L. Williams, R. Payne, R. Roberts, R. Rowe, R. Docherty, Crystal chemistry and solvent effects in polymorphic systems Sulfathiazole, *J. Chem. Soc., Faraday Trans.* 94 (1998) 1035–1045.
- [15] M. Lagas, C.F. Lerk, The polymorphism of sulphathiazole, *Int. J. Pharm.* 8 (1981) 11–24.
- [16] J. Anwar, S.E. Tarling, P. Barnes, Polymorphism of sulfathiazole, *J. Pharm. Sci.* 78 (1989) 337–342.
- [17] F.C. Chan, J. Anwar, R. Cernik, P. Barnes, R.M. Wilson, *Ab initio* structure determination of sulfathiazole polymorph V from synchrotron X-ray powder diffraction data, *J. Appl. Cryst.* 32 (1999) 436–441.
- [18] D.C. Apperley, R.A. Fletton, R.K. Harris, R.W. Lancaster, S. Tavener, T.L. Threlfall, Sulfathiazole polymorphism studied by magic-angle spinning NMR, *J. Pharm. Sci.* 88 (1999) 1275–1280.
- [19] J.A. Zeitler, D.A. Newnham, P.F. Taday, T.L. Threlfall, R.W. Lancaster, R.W. Berg, C.J. Strachan, M. Pepper, K.C. Gordon, T. Rades, Characterization of temperature-induced phase transitions in five polymorphic forms of sulfathiazole by terahertz pulsed spectroscopy and differential scanning calorimetry, *J. Pharm. Sci.* 95 (2006) 2486–2498.
- [20] J.E. Anderson, S. Moore, F. Tarczynski, D. Walker, Determination of the onset of crystallization of N1-2-(thiazolyl)sulfanilamide (sulfathiazole) by UV-Vis and calorimetry using an automated reaction platform; subsequent characterization of polymorphic forms using dispersive Raman spectroscopy, *Spectrochim. Acta Part A* 57 (2001) 1793–1808.

- [21] M.M. Parmar, O. Khan, L. Seton, J.L. Ford, Polymorph selection with morphology control using solvents, *Cryst. Growth Design* 7 (2007) 1635–1642.
- [22] K. Pöllänen, A. Häkkinen, M. Huhtanen, S.-P. Reinikainen, M. Karjalainen, J. Rantanen, M. Louhi-Kultanen, L. Nyström, DRIFT-IR for quantitative characterization of polymorphic composition of sulfathiazole, *Anal. Chim. Acta* 544 (2005) 108–117.
- [23] K. Pöllänen, A. Häkkinen, S.-P. Reinikainen, J. Rantanen, M. Karjalainen, M. Louhi-Kultanen, L. Nyström, IR spectroscopy together with multivariate data analysis as a process analytical tool for in-line monitoring of crystallization process and solid-state analysis of crystalline product, *J. Pharm. Biomed. Anal.* 38 (2005) 275–284.
- [24] J. Aaltonen, J. Rantanen, S. Siirä, M. Karjalainen, A. Jørgensen, N. Laitinen, M. Savolainen, P. Seitavuopio, M. Louhi-Kultanen, J. Yliruusi, Polymorph screening using near-infrared spectroscopy, *Anal. Chem.* 75 (2003) 5267–5273.
- [25] P.E. Luner, S. Majuru, J.J. Seyer, M.S. Kemper, Quantifying crystalline form composition in binary powder mixtures using near-infrared reflectance spectroscopy, *Pharm. Dev. Technol.* 5 (2000) 231–246.
- [26] A.D. Patel, P.E. Luner, M.S. Kemper, Low-level determination of polymorph composition in physical mixtures by near-infrared reflectance spectroscopy, *J. Pharm. Sci.* 90 (2001) 360–370.
- [27] A. Heinz, M. Savolainen, T. Rades, C.J. Strachan, Quantifying ternary mixtures of different solid-state forms of indomethacin by Raman and near-infrared spectroscopy, *Eur. J. Pharm. Sci.* 32 (2007) 182–192.
- [28] N. Chieng, S. Rehder, D. Saville, T. Rades, J. Aaltonen, Quantitative solid-state analysis of three solid forms of ranitidine hydrochloride in ternary mixtures using Raman spectroscopy and X-ray powder diffraction, *J. Pharm. Biomed. Anal.* 49 (2009) 18–25.
- [29] <http://www.nuigalway.ie/cryst/software.html>.
- [30] P. McArdle, K. Gilligan, D. Cunningham, R. Dark, M. Mahon, A method for the prediction of the crystal structure of ionic organic compounds—the crystal structures of *o*-toluidinium chloride and bromide and polymorphism of bicifadine hydrochloride, *CrystEngComm* 6 (2004) 303–309.
- [31] A. Alex, P.C. Granovsky, GAMESS/Firefly version 7.1.F, <http://classic.chem.msu.edu/gran/gamess/index.html>.
- [32] M.W. Schmidt, K.K. Baldrige, J.A. Boatz, S.T. Elbert, M.S. Gordon, J.H. Jensen, S. Koseki, N. Matsunaga, K.A. Nguyen, S. Su, T.L. Windus, M. Dupuis, J.A. Montgomery, General atomic and molecular electronic structure system, *J. Comput. Chem.* 14 (1993) 1347–1363.
- [33] A. Salari, R.E. Young, Application of attenuated total reflectance FTIR spectroscopy to the analysis of mixtures of pharmaceutical polymorphs, *Int. J. Pharm.* 163 (1998) 157–166.
- [34] H.R.H. Ali, H.G.M. Edwards, I.J. Scowen, Insight into thermally induced solid-state polymorphic transformation of sulfathiazole using simultaneous *in situ* Raman spectroscopy and differential scanning calorimetry, *J. Raman Spectrosc.* 40 (2009) 887–892.
- [35] P. McArdle, K. Gilligan, D. Cunningham, A.G. Ryder, Determination of the polymorphic forms of bicifadine hydrochloride by differential scanning calorimetry-thermogravimetric analysis, X-ray powder diffraction, attenuated total reflectance-infrared spectroscopy, and attenuated total reflectance-near-infrared spectroscopy, *Appl. Spectrosc.* 59 (2005) 1365–1371.
- [36] Y. Xie, W. Cao, S. Krishnan, R. Chiu, H. Li, N. Cauchon, Characterization of mannitol polymorphic forms in lyophilized protein formulations using a multivariate curve resolution (MCR)-based Raman spectroscopic method, *Pharm. Res.* 25 (2008) 2292–2301.
- [37] I.S. Lee, A.Y. Lee, A.S. Myerson, Concomitant polymorphism in confined environment, *Pharm. Res.* 25 (2008) 960–968.
- [38] S. Wold, H. Antti, F. Lindgren, J. Öhman, Orthogonal signal correction of near-infrared spectra, *Chemom. Intell. Lab. Syst.* 44 (1998) 175–185.
- [39] L. Xie, Y. Ying, T. Ying, Rapid determination of ethylene content in tomatoes using visible and short-wave near-infrared spectroscopy and wavelength selection, *Chemom. Intell. Lab. Syst.* 97 (2009) 141–145.
- [40] M.S. Dhanoa, S.J. Lister, R. Sanderson, R.J. Barnes, The link between multiplicative scatter correction (MSC) and standard normal variate (SNV) transformations of NIR spectra, *J. Near Infrared Spectrosc.* 2 (1994) 43–47.
- [41] I.S. Helland, T. Naes, T. Isaksson, Related versions of the multiplicative scatter correction method for preprocessing spectroscopic data, *Chemom. Intell. Lab. Syst.* 29 (1995) 233–241.
- [42] M. Tiwari, G. Chawla, A.K. Bansal, Quantification of olanzapine polymorphs using powder X-ray diffraction technique, *J. Pharm. Biomed. Anal.* 43 (2007) 865–872.
- [43] Y. Xie, W. Tao, H. Morrison, R. Chiu, J. Jona, J. Fang, N. Cauchon, Quantitative determination of solid-state forms of a pharmaceutical development compound in drug substance and tablets, *Int. J. Pharm.* 362 (2008) 29–36.
- [44] ICH Harmonized guideline, 1996. Q2B: Note for Guidance on Validation of Analytical Procedures: Methodology.
- [45] S.N. Campbell Roberts, A.C. Williams, I.M. Grimsey, S.W. Booth, Quantitative analysis of mannitol polymorphs. X-ray powder diffractometry—exploring preferred orientation effects, *J. Pharm. Biomed. Anal.* 28 (2002) 1149–1159.
- [46] K. Kachrimanis, M. Rontogianni, S. Malamataris, Simultaneous quantitative analysis of mebendazole polymorphs A–C in powder mixtures by DRIFTS spectroscopy and ANN modeling, *J. Pharm. Biomed. Anal.* 51 (2010) 512–520.